Advancement in Scientific and Engineering Research
Vol. 2(3), pp. 48-61, September 2014
ISSN: 2384-7336
Research Paper

Internal wave exciting force on a rectangular barge in a two-layer fluid of finite depth

Manyanga O. David[1*] • Duan Wen-yang[2] • Han Xuliang[2] • Cheng Ping[2]

[1]Mathematics Department, Egerton University, 536-20115, Egerton-Njoro, Kenya.
[2]College of Shipbuilding Engineering, Harbin Engineering University, Harbin 150001, China.

*Corresponding author. E-mail: davondiek@yahoo.com.

Accepted 12th June, 2014

Abstract. Internal waves may greatly affect the hydrodynamics of a body performing in a stratified fluid. The internal waves may occur due to density difference of a fluid having layers with different temperatures in the vertical sense or salinity. In such cases, the waves perform differently in each layer, depending on the wave mode. Consequently, the wave loads such as the wave exciting forces will vary greatly. To study these phenomena, one can model a two-layer fluid with free surface and a rigid bottom. In such a fluid, there are two modes of motion due to the surface waves and internal waves. The former is referred to as the surface wave mode while the latter is internal wave mode. For these two modes, the wave exciting forces are of great interest to study. Presently, no one has clearly solved three dimensional internal wave exciting forces for a two-layer fluid of finite depth. The present work has solved internal wave forces for the body floating in the upper layer and lower layer of a two-layer fluid of finite depth. Green functions are used to obtain the radiation potential, together with the incidence wave potential to calculate the wave exciting forces. A boundary integral equation method together with the Green's theorem is used to get the velocity potential on the wetted surface of the body. The advantage of the method is that it involves integration once to obtain the pressure forces and in a similar manner the velocity potential required. The present work is very applicable in the design of the off shore structures and constructions taking place in shallowly stratified fluids.

Keywords: Internal waves, wave exciting force, Green functions, velocity potential.

Nomenclature: $\phi_{(1)}$, velocity potential in the upper layer; $\phi_{(2)}$, velocity potential in the lower layer; σ, frequency of oscillation; g, acceleration due to gravity; $\rho_{(1)}$, density of fluid of the upper layer; $\rho_{(2)}$, density of fluid of the lower layer; γ, density ratio; $G^{(1)}$, Green function in the upper layer; $G^{(2)}$, Green function in the lower layer; p, field point; q, source point; α angle of wave incidence; η, wave elevation; n, normal vector directed inward domain.

INTRODUCTION

Wave exciting forces have been studied extensively in a fluid of uniform density, single layer cases. The stratified fluid case has received little attention. Recently, Mohapatra and Bora (2008) studied the wave exciting forces on a sphere in a two-layer fluid. They used the method of multipole expansion to obtain their radiation potential. However, they did not study the influence of internal waves on the wave exciting forces; they only looked at the cases similar to those of single layer. Nguyen and Yeung (2010) studied the influences of the density ratio and variation of lower layer depth on the wave exciting forces on a floating barge. However, they used the source distribution method which involves integration more than once to obtain the radiation potential.

On the other hand, they only considered a body floating in the upper layer and not touching the interface. Ten and Kashiwagi (2004) studied radiation problems of a general body in a two-layer fluid of finite depth. They used a boundary integral equation method to obtain the velocity potential on the wetted surface of the body. However, they considered two-dimensional case and the numerical results were for the case of a body floating in the upper layer only. Kashiwagi et al. (2006) applied the same boundary integral equations to obtain and solve the diffraction problems directly. A two-dimensional case was considered again, for a body in the upper and lower layer and the influence of density ratio and the position of the interface were studied. On the other hand, Ying et al. (2012) considered the diffraction for a three dimensional body floating in a two-layer fluid. They used the boundary element method in time domain, and got similar results in the frequency domain. However, like other above mentioned researchers, they only considered the body in the upper layer.

It is also important to note that the density ratio effects are of importance in the diffraction predictions, since the forces depend on waves. There is a need to know about wave characteristics in order to understand their influences on these forces. Lu and Chen (2009) have studied both surface and interfacial waves in a two-layer fluid. The wave characteristics they have given are very essential in the analysis of the internal wave excitations. On the other hand, Manyanga and Duan (2011a) have also presented the internal wave amplitudes and how they are influenced by the density ratio in a two-layer fluid of finite depth. An extension on this analysis has been carried out by Manyanga and Duan (2012) to study the aspects of velocity and acceleration, among other wave properties. This is important since a force is proportional to the acceleration due to the fluid motion. Some of these aspects have also been studied extensively by Grue et al. (1999) and Grue and Jensen (2006). Their experimental results are very intuitive in understanding the internal wave influence on the wave force on a floating body.

In this paper, we consider the influence of internal waves on the exciting forces for a three dimensional body, heaving either in the upper or lower layer of a two-layer fluid of finite depth. The method of boundary integral equations is used, together with the Green's theorem to obtain the radiation potential on the wetted body surface of a rectangular floating barge. This method provides a straight forward way to integrate the radiation pressure from the linear Bernoulli equation to get the required potential. To do this the appropriate Green functions, as in Manyanga and Duan (2011b) have been used. These Green functions have been proved to be robust and time saving in computer memory. In this case, the surface integration is done by the panel method following Hess and Smith (1964). After obtaining the radiation potential, the dynamic force and Froud Kriloff force are calculated, and consequently the wave exciting force. For each case of the layers, incidence wave potentials are derived, since they are necessary for the evaluation of the diffraction potentials.

MATHEMATICAL FORMULATIONS

Consider a uniform rectangular box in a two-layer fluid of finite depth. Boundary integral equations are derived for the cases when it is floating in the upper or lower layer, respectively. To do this, the following kinematics and body boundary conditions must be fulfilled by a velocity potential. This velocity potential is obtained by appropriate Green functions and applying the Greens second identity. So, let the box be at the interface of the fluid domain, as in Figure 1. Suppose the box in calm water and is given some small angular frequency ω then the free surface, interface and the bottom boundary conditions become:

$$\frac{\partial \phi^{(1)}}{\partial y} - \nu\phi^{(1)} = 0, \quad y = h_1, \ \nu = \frac{\sigma^2}{g} \tag{1}$$

$$\gamma\left(\frac{\partial \phi^{(1)}}{\partial y} - \nu\phi^{(1)}\right) = \frac{\partial \phi^{(2)}}{\partial y} - \nu\phi^{(2)}, \qquad y = 0, \ \gamma = \frac{\rho_1}{\rho_2} \tag{2}$$

$$\frac{\partial \phi^{(1)}}{\partial y} = \frac{\partial \phi^{(2)}}{\partial y}, \qquad y = 0 \tag{3}$$

$$\frac{\partial \phi^{(2)}}{\partial y} = 0, \qquad y = -h_2 \tag{4}$$

Let the functions ϕ and G be harmonic in a closed region by the contour S, and the function G has a singular behavior at *P*. The aim is to obtain ϕ (the velocity potential) given an appropriate Green function, G by applying the Green's theorem. Then for n-normal vector directed inward the domain, we have the integral equation to be solved in the form,

$$b(p)\phi(p) = \int_S \left(\phi\frac{\partial G}{\partial n} - G\frac{\partial \phi}{\partial n}\right)ds = \begin{cases} 0, & p \text{ outside } S \\ -2\pi\phi(p), & p \text{ on } S \\ -4\pi\phi(p), & p \text{ inside } S \end{cases} \tag{5}$$

Now, on the free surface, the normal derivative is congruent to the direction of the derivative with respect to *y*, which can be obtained from the boundary condition (Equation 1) in the form:

$$\frac{\partial \phi}{\partial n} = \frac{\partial \phi}{\partial y} = \nu\phi, \qquad \frac{\partial G}{\partial n} = \frac{\partial G}{\partial y} = \nu G \tag{6}$$

Two cases arise in solving the potential in a two-layer

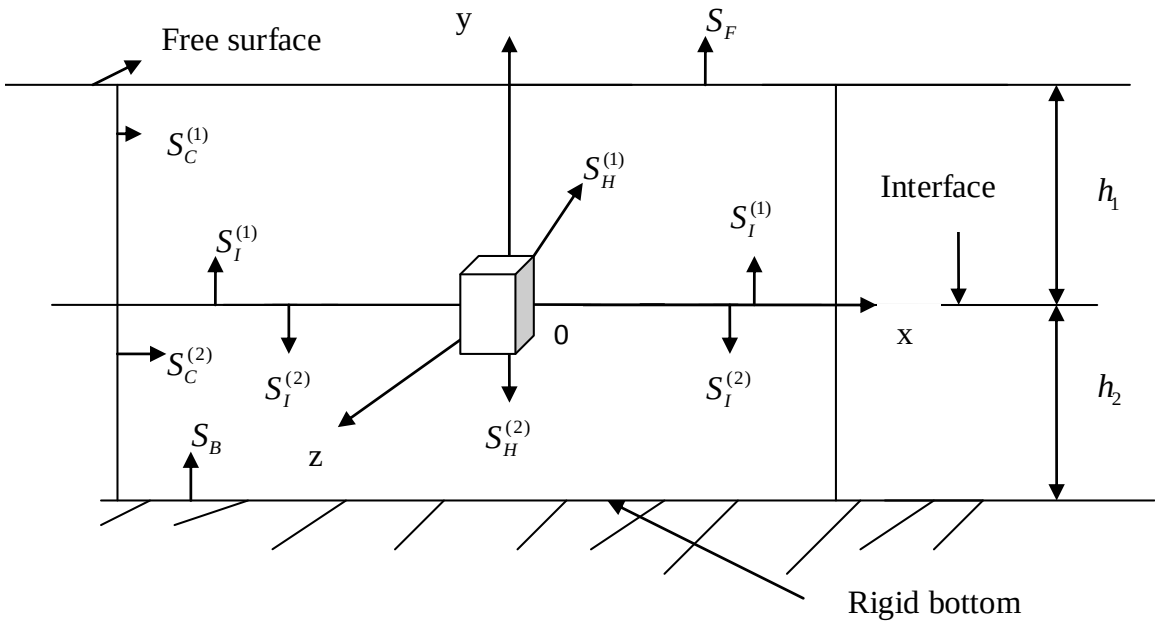

Figure 1. Schematic for the boundary surfaces. $S_H \rightarrow$ The whole wetted surface of the body; $S_H^{(1)}$ *and* $S_H^{(2)} \rightarrow$ Surfaces for the upper- and lower-layer fluid domains, respectively; $S_F \rightarrow$ Free surface; $S_I^{(1)} \rightarrow$ Interface upwards (upper layer); $S_I^{(2)} \rightarrow$ Interface downwards (lower layer); $S_B \rightarrow$ Rigid bottom; $S_C^{(1)} \rightarrow$ Control surface for upper region; $S_C^{(2)} \rightarrow$ Control surface for lower region.

fluid, that is, when the body is floating in the upper layer and when in the lower layer. Care should be taken when deriving such a potential at the interface. In the present method, the interface is considered to be continuous across the layers hence the potential is also continuous.

Upper layer case

Let the box be located in the upper layer of the two-layer fluid, then from Equations 5 and 6, applying the Green's theorem in both domains yield:

$$b(p)\phi^{(1)}(p) = \iint_{S_1}\left(\phi^{(1)}(q)\frac{\partial G^{(1)}(q:p)}{\partial n(q)} - G^{(1)}(q:p)\frac{\partial \phi^{(1)}(q)}{\partial n(q)}\right)dS(q) \quad (7)$$

$$0 = \iint_{S_2}\left(\phi^{(2)}(q)\frac{\partial G^{(2)}(q:p)}{\partial n(q)} - G^{(2)}(q:p)\frac{\partial \phi^{(2)}(q)}{\partial n(q)}\right)dS(q) \quad (8)$$

Using the properties of the boundary surfaces above and mathematical manipulations give the boundary integral equation to be solved as:

$$b(p)\phi^{(1)}(p) = \iint_{S_H^{(1)}}\left(\phi^{(1)}\frac{\partial G^{(1)}}{\partial n} - G^{(1)}\frac{\partial \phi^{(1)}}{\partial n}\right)dS + \frac{1}{\gamma}\iint_{S_H^{(2)}}\left(\phi^{(2)}\frac{\partial G^{(2)}}{\partial n} - G^{(2)}\frac{\partial \phi^{(2)}}{\partial n}\right)dS \quad (9)$$

Lower layer case

In a similar way to the body located in the upper layer case, we apply Green's theorem to both the upper layer and lower layer domains. Thus from Equations 5 and 6, we have:

$$0 = \iint_{S_1}\left(\phi^{(1)}(q)\frac{\partial G^{(1)}(q:p)}{\partial n(q)} - G^{(1)}(q:p)\frac{\partial \phi^{(1)}(q)}{\partial n(q)}\right)dS(q) \quad (10)$$

$$b(p)\phi^{(2)}(p) = \iint_{S_2}\left(\phi^{(2)}(q)\frac{\partial G^{(2)}(q:p)}{\partial n(q)} - G^{(2)}(q:p)\frac{\partial \phi^{(2)}(q)}{\partial n(q)}\right)dS(q) \quad (11)$$

Again using the properties of the boundary surfaces above and after some mathematical manipulations gives the boundary integral equation to be solved as:

$$b(p)\phi^{(2)}(p) = \gamma\iint_{S_H^{(1)}}\left(\phi^{(1)}\frac{\partial G^{(1)}}{\partial n} - G^{(1)}\frac{\partial \phi^{(1)}}{\partial n}\right)dS + \iint_{S_H^{(2)}}\left(\phi^{(2)}\frac{\partial G^{(2)}}{\partial n} - G^{(2)}\frac{\partial \phi^{(2)}}{\partial n}\right)dS \quad (12)$$

Numerical solutions

Consider the first integral part of Equation 9:

$$\iint_{S_H^{(1)}} \left(\phi^{(1)} \frac{\partial G^{(1)}}{\partial n} - G^{(1)} \frac{\partial \phi^{(1)}}{\partial n} \right) dS \tag{13}$$

For $S_H^{(1)}$ is the enclosing surface, we discretise it into N-quadrilateral elements (N-panels) to approximate the body surface.
Let

$$\left.\begin{aligned} A_{i,j} &= \frac{1}{2\pi} \iint_{S_H^{(1)}} \frac{\partial G^{(1)}}{\partial n} ds_{j,} \qquad \text{in } the\ j^{th}\ element \\ B_{i,j} &= \frac{1}{2\pi} \iint_{S_H^{(1)}} G^{(1)} n_j ds_{j,} \qquad \text{in } the\ j^{th}\ element \end{aligned}\right\} \tag{14}$$

We take $\phi_j^{(1)}$ to be a constant potential in the j^{th} element. Thus, $\frac{\partial \phi_j^{(1)}}{\partial n_j}$ is also constant in the j^{th} element. Hence, we have:

$$\sum_{j=1}^{N} A_{i,j} \phi_j^{(1)} = C_i \tag{15}$$

Equation 15 is a system of linear equations to be solved for $\phi_j^{(1)}$, by the methods of Hess and Smith (1964).

Note that:
N = number of quadrilateral elements

$$A_{i,j} = 2\pi \qquad i = j$$

$$= \frac{1}{2\pi} \iint_{H^{(1)}} n_j \square \nabla G^{(1)} ds_j \qquad i \neq j$$

$$C_i = \sum_{j=1}^{N} B_{i,j}$$

n_j = the generalized unit normal in the j^{th} direction

INCIDENCE WAVE POTENTIAL

The incidence wave velocity potentials are very important for the analysis of the plane progressive waves. For a single layer case, these potentials have been derived. However, in a two-layer fluid, there are two waves of incidence due to the surface wave mode and interface wave mode. These waves progress with different wavelengths as has been discussed in details by Manyanga and Duan (2012). We need these potentials in order to calculate the wave exciting forces.

We define the velocity potential $\Phi^{(m)}$ of the general incidence wave as:

$$\Phi^{(1)} = \mathrm{Re}\left\{ A_0 \left(k \cosh k(y - h_1) + v \sinh k(y - h_1) \right) \times e^{i\left[k(x\cos\alpha + z\sin\alpha) + \sigma t \right]} \right\} \tag{16}$$

$$\Phi^{(2)} = \mathrm{Re}\left\{ B_0 \cosh k(y + h_2) e^{i\left[k(x\cos\alpha + z\sin\alpha) + \sigma t \right]} \right\} \tag{17}$$

The above potentials must satisfy the Laplace equation, kinematics and dynamic conditions on the free surface and interface and also the bottom conditions, as below:

$$\nabla \Phi^{(m)} = 0, \qquad m = 1, 2 \tag{18}$$

$$\frac{\partial \Phi^{(1)}}{\partial y} - \frac{\partial \eta^{(1)}}{\partial t} = 0, \qquad y = h_1 \tag{19}$$

$$\frac{\partial \Phi^{(1)}}{\partial t} + g\eta^{(1)} = 0, \qquad y = h_1 \tag{20}$$

$$\frac{\partial \Phi^{(1)}}{\partial y} = \frac{\partial \Phi^{(2)}}{\partial y} = \frac{\partial \eta^{(2)}}{\partial t}, \qquad y = 0 \tag{21}$$

$$\gamma \left(\frac{\partial \Phi^{(1)}}{\partial t} + g\eta^{(1)} \right) = \frac{\partial \Phi^{(2)}}{\partial t} + g\eta^{(2)}, \qquad y = 0 \tag{22}$$

$$\frac{\partial \Phi^{(2)}}{\partial y} = 0, \qquad y = -h_2 \tag{23}$$

Besides this, define the surface and interface elevations for the waves as:

$$\eta^{(m)}(x, z, t) = \mathrm{Re}\left\{ a^{(m)} e^{i\left[k(x\cos\alpha + z\sin\alpha) + \sigma t \right]} \right\}, \ m = 1, 2 \tag{24}$$

where $a^{(1)}$ and $a^{(2)}$ are the amplitudes of the surface and internal waves, respectively. Substituting Equation 16 together with Equation 24 into the free surface boundary condition (Equation 20), we get:

$$A_o = \frac{iga^{(1)}}{\sigma k} \tag{25}$$

Similarly, substituting Equations 16 and 17 together with Equation 25 and $\eta^{(2)}$ into the interface kinematic boundary condition (Equation 20), we obtain:

$$B_o = \frac{iga^{(1)}}{k\sinh kh_2} \tag{26}$$

Thus, we can write the surface incidence velocity potential as:

$$\Phi^{(1)} = \mathrm{Re}\left\{\frac{iga^{(1)}}{\sigma k}\left(k\cosh k(y-h_1)+v\sinh k(y-h_1)\right)\times e^{i\left[k(x\cos\alpha+z\sin\alpha)+\sigma t\right]}\right\} \tag{27}$$

$$\Phi^{(2)} = \mathrm{Re}\left\{\frac{iga^{(1)}}{k\sinh kh_2}\cosh k(y+h_2)e^{i\left[k(x\cos\alpha+z\sin\alpha)+\sigma t\right]}\right\} \tag{28}$$

Now, in order to obtain the incidence velocity potential of the internal waves, we substitute Equations 25 and 26 into Equation 20, this gives:

$$a^{(1)} = \frac{\sigma^2 a^{(2)}}{\left(\sigma^2 - gk\tanh kh_1\right)\cosh kh_1} \tag{29}$$

Hence, we can express the incidence wave potential of the internal waves as:

$$\Phi^{(1)} = \mathrm{Re}\left\{\frac{ig\sigma a^{(2)}\left(k\cosh k(y-h_1)+v\sinh k(y-h_1)\right)}{k\left(\sigma^2 - gk\tanh kh_1\right)\cosh kh_1}\times \right. \tag{30}$$

$$\left. \times e^{i\left[k(x\cos\alpha+z\sin\alpha)+\sigma t\right]}\right\}$$

$$\Phi^{(2)} = \mathrm{Re}\left\{\frac{ig\sigma^2 a^{(2)}\cosh k(y+h_2)}{k\left(\sigma^2 - gk\tanh kh_1\right)\cosh kh_1\sinh kh_2}\times e^{i\left[k(x\cos\alpha+z\sin\alpha)+\sigma t\right]}\right\} \tag{31}$$

HYDRODYNAMIC FORCES

Now we can derive the wave forces and loads using the incidence velocity potentials and the radiation potential. We define the total velocity potential on the body, Φ depending on whether the body is in the upper or lower layer, as:

$$\Phi^{(m)} = \phi_0^{(m)} + \sum_{j=1}^{6}\phi_j^{(m)} + \phi_7^{(m)} \tag{32}$$

Where m = 1, 2 refers to upper and lower layers, respectively, $\phi_0^{(m)}$ is the incidence velocity potential, $\phi_j^{(m)}$ is the radiation potentials related to the body motion in calm water (where j denotes the mode of motion) $\phi_7^{(m)}$ is the scattering or diffraction potential corresponding to the restrained body in its mean position.

The assumption of small amplitude motion allows the kinematics boundary condition on the immersed surface of the body to be satisfied in its mean position, that is:

$$\frac{\partial\phi_j}{\partial n} = n_j \text{ ,j=1, 2… 6} \tag{33}$$

$$\frac{\partial\phi_0}{\partial n} = -\frac{\partial\phi_7}{\partial n} = n_7 \tag{34}$$

Where, generally,

$n_1 = n_x, \quad n_2 = n_y, \quad n_3 = n_z$

$n_4 = yn_z - zn_y, \quad n_5 = zn_x - xn_z, \quad n_6 = xn_y - yn_x$

The hydrodynamic force and momentum acting on a body can be defined as:

$$\vec{F}_j = \int_S P\vec{n}_j ds \text{ , } \quad j=1, 2, 3 \tag{35}$$

$$\vec{M}_j = \int_S P(\vec{r}-\vec{r}_g)\times\vec{n}_j ds \text{ , } \quad j=4, 5, 6 \tag{36}$$

Here P is the fluid pressure that can be obtained from Euler's integral as:

$$P = \mathrm{Re}\left\{\sum_{j=0}^{7}\rho_m\sigma^2 a_i^{(m)}\phi_j^{(m)}e^{(-i\sigma_{(l)}t)}\right\} \tag{37}$$

Where, ρ_m is the density of the fluid, either in the upper or lower layer depending on the value of m, σ is the frequency of oscillation and $a_i^{(m)}$ is the complex wave amplitude. Hence we can rewrite the force and moment in Equations 35 and 36 using Equation 37 as:

$$\vec{F} = \mathrm{Re}\left\{\sum_{j=0}^{7}\rho_m\sigma^2 a_i^{(m)}e^{(-i\sigma_{(l)}t)}\int_S\phi_j^{(m)}\vec{n}ds\right\} \tag{38}$$

$$\vec{M} = \left\{\sum_{j=0}^{7}\rho_m\sigma^2 a_i^{(m)}e^{(-i\sigma_{(l)}t)}\int_S\phi_j^{(m)}(\vec{r}-\vec{r}_g)\times\vec{n}ds\right\} \tag{39}$$

Let's denote $\vec{f} = f_1\hat{i} + f_2\hat{j} + f_3\hat{k}$ and $\vec{m} = f_4\hat{i} + f_5\hat{j} + f_6\hat{k}$, then we can now write the complex hydrodynamic force and moment as:

$$f_k = \sum_{j=0}^{7} \rho_m \sigma^2 a_i^{(m)} \int_S \phi_j^{(m)} n_k ds\,, \quad k = 1,2...6 \tag{40}$$

WAVE EXCITING FORCE

The wave exciting force can be obtained from Equation 40 by redefining it into the radiation and diffraction force parts. We now derive it here for the case when the body floats in upper layer first; the other cases follow immediately in a similar manner.
For a body floating freely in calm water, it relies on the incident wave. Let,

$$\Phi^{(1)} = \phi_0^{(1)} + \phi_7^{(1)} \tag{41}$$

where the $\phi_0^{(1)}$ and $\phi_7^{(1)}$ have been defined earlier, as incidence and diffraction potentials, respectively.

Note that the potential $\phi_0^{(1)}$ satisfies the free surface and interface boundary conditions (Equations 18 to 23), while the potential $\phi_7^{(1)}$ satisfies the radiation condition:

$$\underset{R\to\infty}{Lim}\ \phi_7^{(1)} = 0 \tag{42}$$

Assume that $\phi_7^{(1)}$ is known, and $\phi_0^{(1)}$ is given from Equation 27, then:

$$\Phi^{(1)} = \phi_0^{(1)} + \phi_7^{(1)} \tag{43}$$

So, $\phi^{(1)}$ is known and we can now calculate the dynamic pressure from the linear terms of Bernoulli equation:

$$P^{(1)} = -\rho_1 \frac{\partial \Phi^{(1)}}{\partial t} = -\rho_1 \frac{\partial \phi_0^{(1)}}{\partial t} - \rho_1 \frac{\partial \phi_7^{(1)}}{\partial t} \tag{44}$$

Hence the dynamic force is:

$$\vec{F}^{(1)} = \int_{S_H^{(1)}} -\vec{n} P^{(1)} ds \tag{45}$$

$$= \int_{S_H^{(1)}} \rho_1 \frac{\partial \phi_0^{(1)}}{\partial t} \vec{n} ds + \int_{S_H^{(1)}} \rho_1 \frac{\partial \phi_7^{(1)}}{\partial t} \vec{n} ds \tag{46}$$

Equation 46 contains the Froud Krillof force and the Diffraction force, first and second parts, respectively.

We first derive the diffraction force as follows:

$$\vec{F}_D^{(1)} = \int_{S_H^{(1)}} \rho_1 \frac{\partial \phi_7^{(1)}}{\partial t} \vec{n} ds$$

$$= \int_{S_H^{(1)}} \rho_1 \frac{\partial \phi_7^{(1)}}{\partial t} \frac{\partial \phi_k^{(1)}}{\partial n} ds \tag{47}$$

$$= i\rho_1 \sigma \int_{S_H^{(1)}} \phi_7^{(1)} \frac{\partial \phi_k^{(1)}}{\partial n} ds$$

Due to the symmetry property

$$\vec{F}_D^{(1)} = i\rho_1 \sigma \int_{S_H^{(1)}} \phi_k^{(1)} \frac{\partial \phi_7^{(1)}}{\partial n} ds \tag{48}$$

But we have that,

$$\frac{\partial \phi_7^{(1)}}{\partial n} = -\frac{\partial \phi_0^{(1)}}{\partial n} \tag{49}$$

Consequently, the diffraction force becomes:

$$\vec{F}_D^{(1)} = -i\rho_1 \sigma \int_{S_H^{(1)}} \phi_k^{(1)} \frac{\partial \phi_0^{(1)}}{\partial n} ds, \quad k = 1,2,...6 \tag{50}$$

Now we calculate the Froud Krillof force. This is defined as:

$$\vec{F}_{FK}^{(1)} = \int_{S_H^{(1)}} -\rho_1 \frac{\partial \phi_0^{(1)}}{\partial t} (-\vec{n}) ds \tag{51}$$

From Equation 27 we get:

$$\frac{\partial \phi_0^{(1)}}{\partial t} = i\sigma \phi_0^{(1)} \tag{52}$$

Thus, using Equation 52 in Equation 41 gives:

$$\vec{F}_{FK}^{(1)} = \int_{S_H^{(1)}} i\rho_1 \sigma \phi_0^{(1)} \vec{n} ds$$

$$= i\rho_1 \sigma \int_{S_H^{(1)}} \phi_0^{(1)} \frac{\partial \phi_k^{(1)}}{\partial n} ds \tag{53}$$

Hence, the wave exciting force for a body floating in the

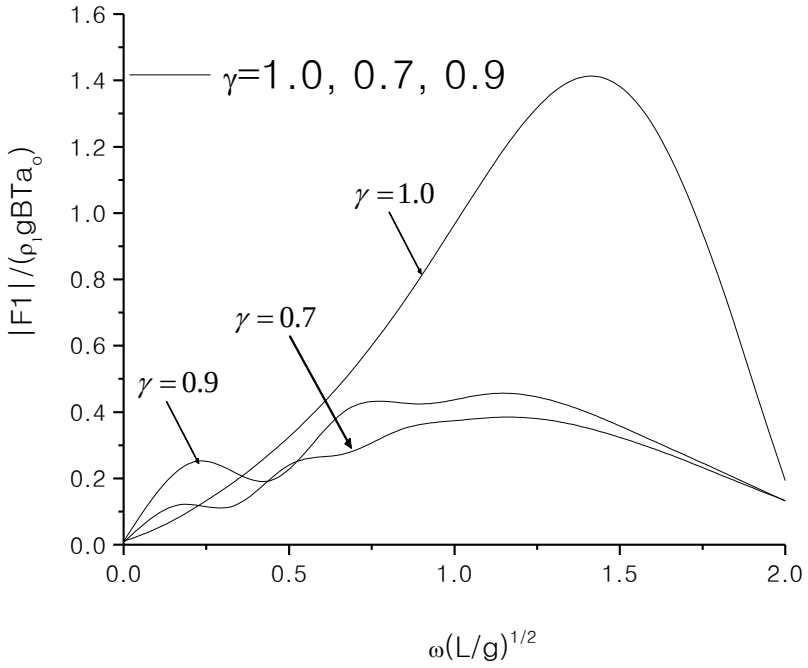

Figure 2. Magnitude of surge wave exciting force of a box, upper layer ($h_1/T=1.2$, $h_2/T=0.4$).

upper layer for a two-layer fluid of finite depth is:

$$\vec{F}_{E,k}^{(1)} = \vec{F}_{FK}^{(1)} + \vec{F}_{D}^{(1)}$$

$$= i\rho_1\sigma \int_{S_H^{(1)}} \left(\phi_0^{(1)} \frac{\partial \phi_k^{(1)}}{\partial n} - \phi_k^{(1)} \frac{\partial \phi_0^{(1)}}{\partial n} \right) ds \quad (54)$$

The wave exciting force for a body floating in the lower layer is obtained in a similar way.

RESULTS AND DISCUSSION

In the present method, a rectangular box is used to obtain the wave excitation force due to incidence waves. The dimensions of the box were taken as; Length, L = 2.25 m; Breadth, B = 2.25 m; and Draught, T = 1.00 m. Two cases were considered in the numerical calculations, when the box is in the upper layer and when the box is in the lower layer. For each case, the influences of the density ratio and the position of the interface were analyzed and presented.

Upper layer case

For this case, to study the influence of the density ratio, the depths were fixed at $h_1/T=1.2$, $h_2/T=0.4$ and $h=h_1+h_2$ for different density ratios $\gamma=0.7, 0.9, 1.0$. In fact for $\gamma=1.0$, the two-layer fluid reduces to those of single layer case with $h/T=1.6$ and numerical results can be compared to those of Endo (1987). The numerical results also show that results for the two-layer and the single layer fluids converge exactly, at this condition. The results for $\gamma=0.7$ *and* 0.9 show the presence of the internal waves, thus they demonstrate the influence of internal waves on the wave exciting forces on the box as can be seen in Figures 2 and 3. They show that at high frequencies, the internal waves are not important and can be ignored, and that the results are comparable to those of single layer case. However, at relatively low frequency there is visible interference of the internal waves. It is also noted that as the density ratio increases, the disturbance becomes larger, as can be seen clearly more in the surge excitation. On the other hand, the interface position greatly affects the wave loads on the floating body in a two- layer fluid. This can be observed by fixing the density ratio at $\gamma=0.9$ and varying the depths of the fluid layers in the following manner: Upper layer depth as; $h_1 = 1.6$, 1.5, 1.4, 1.3, 1.2 while the lower layer depth as; $h_2 = 0.0, 0.1, 0.2, 0.3, 0.4$; and $h/T=1.6$, respectively. The results for $h_2/h_1=0.0$ are for the case of single layer and are included to show the influence of the internal waves. As can be seen in Figures 4 and 5, the depth can greatly affect the internal waves, the magnitude of the wave

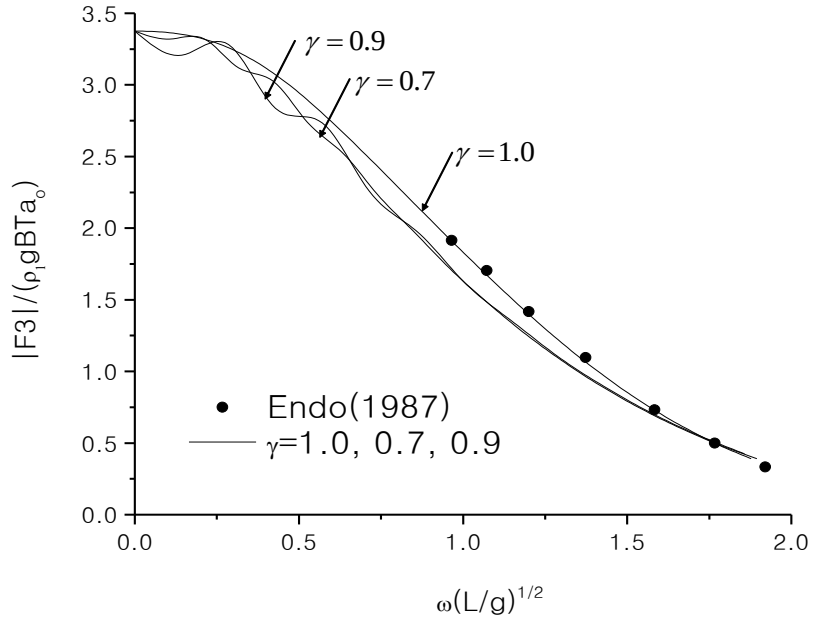

Figure 3. Magnitude of heave wave exciting force of a box, upper layer ($h_1/T=1.2$, $h_2/T=0.4$).

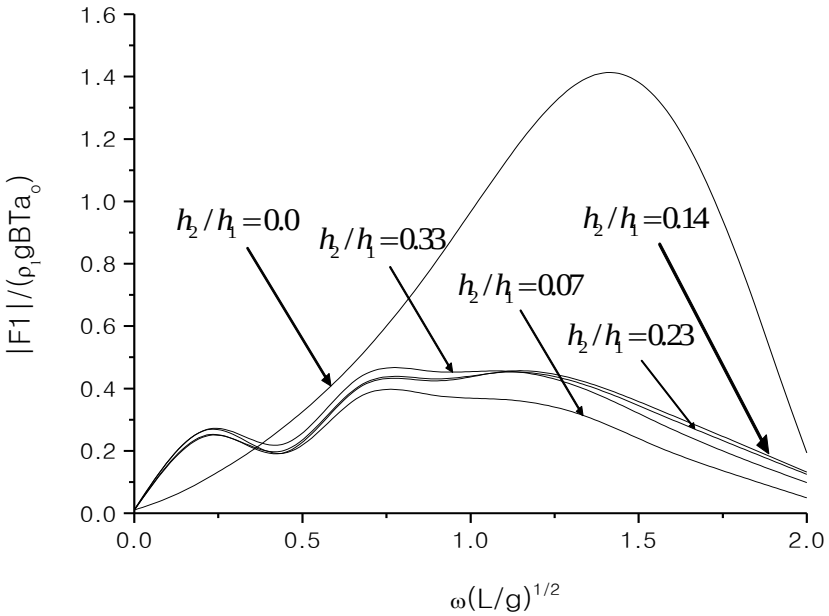

Figure 4. Effects of interface on surge wave exciting force of a box, upper layer, $\gamma=0.9$.

exciting force decreases as the interface is moved upwards.

Lower layer case

In this case, to study the influence of the density ratio, the depths were fixed at $h_1/T=0.4$, $h_2/T=1.2$ and $h=h_1+h_2$ for different density ratios $\gamma=0.0, 0.7, 0.9$. In fact for $\gamma=0.0$, the two-layer fluid reduces to those of single layer case with $h/T=1.6$ and numerical results can be compared to those of single layer cases. The

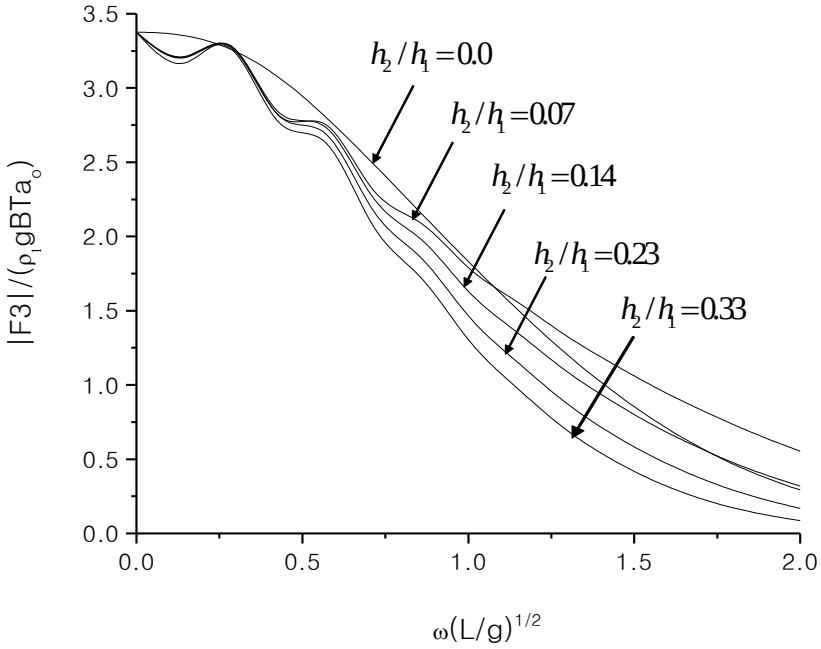

Figure 5. Effects of interface on heave wave exciting force of a box, upper layer, $\gamma = 0.9$.

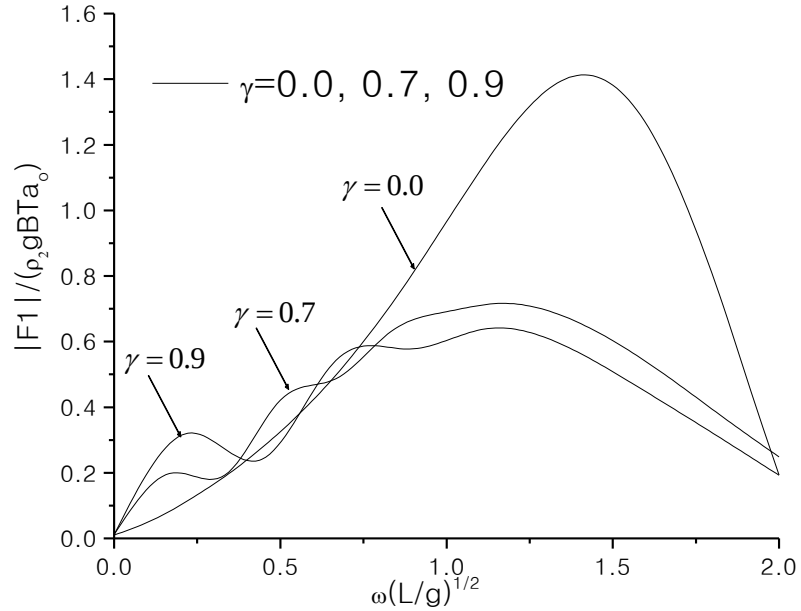

Figure 6. Magnitude of surge wave exciting force of a box, lower layer ($h_1/T = 0.4, h_2/T = 1.2$).

numerical results again show that results for the two-layer and the single layer fluids converge exactly, at this condition. The results for $\gamma = 0.7\ and\ 0.9$ show the presence of the internal waves again, thus they demonstrate the influence of internal waves on the wave exciting forces on the box as can be seen in Figures 6 and 7. They show that at high frequencies, the internal waves are not important and can be ignored, and that the results can be compared to those of single layer case. However, at relatively low frequency, there is visible interference of the internal waves. It is also noted that as the density ratio increases, the disturbance becomes

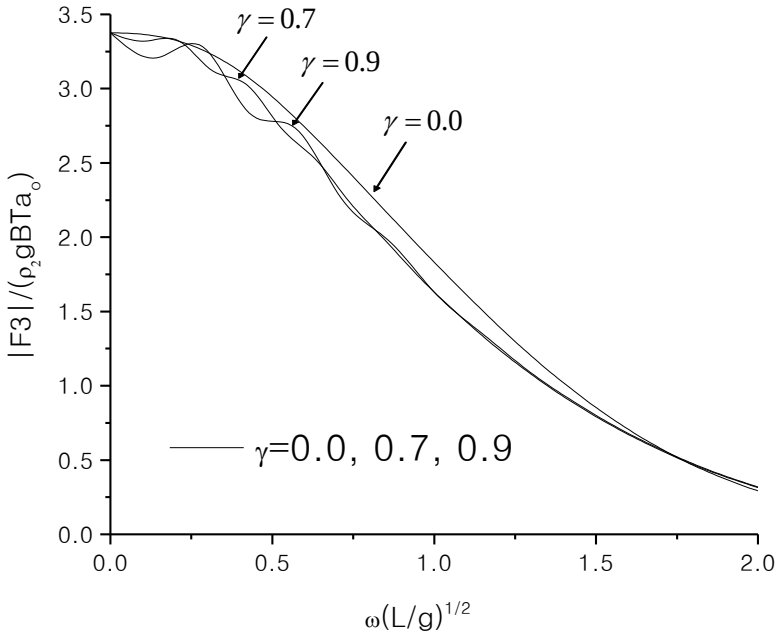

Figure 7. Magnitude of heave wave exciting force of a box, lower layer ($h_1/T=0.4$, $h_2/T=1.2$).

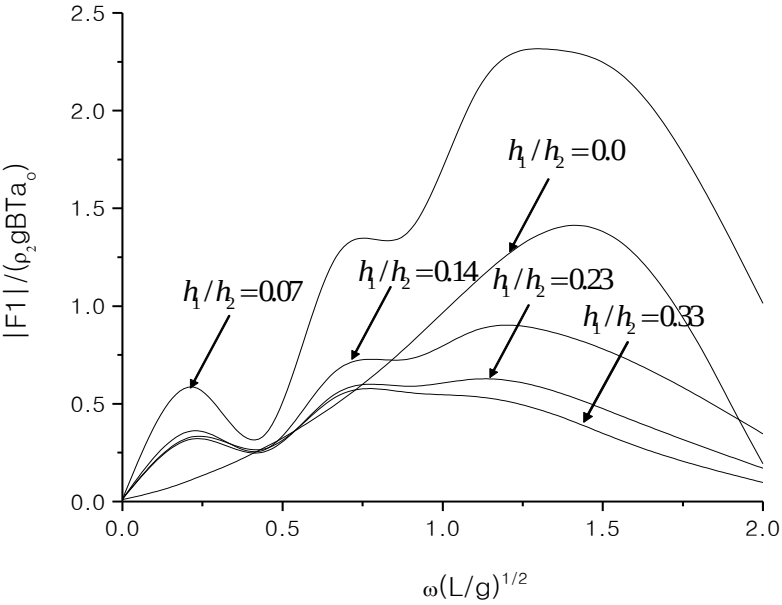

Figure 8. Effects of interface on surge wave exciting force of a box, lower layer, $\gamma=0.9$.

larger, as can be seen clearly more in the surge excitation.

On the other hand, the interface position also greatly affects the wave loads on the floating body in the lower layer of the two-layer fluid. This can be observed by again fixing the density ratio at $\gamma=0.9$ and varying the depths of the fluid layers in the following manner: Upper layer depth as; *h₁/T=0.0, 0.1, 0.2, 0.3* while the lower layer depth as; *h₂/T=1.6, 1.5, 1.4, 1.3, 1.2*, *0.4*; and *h/T=1.6*, respectively. The results for *h₂/h₁=0.0* are for the case of single layer and are included to show the influence of the internal waves. As can be seen in Figures 8 and 9, the depth can greatly affect the internal waves, the magnitude of the wave exciting force decreases

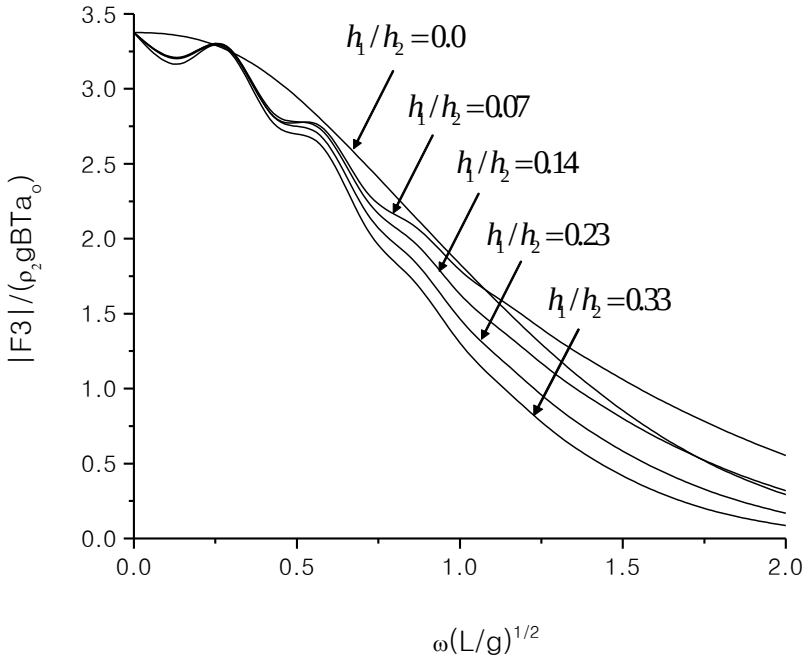

Figure 9. Effects of interface on Heave wave exciting force of a box, lower layer, $\gamma = 0.9$.

as the interface is moved upwards.

CONCLUSIONS

The boundary integral equations for a radiation potential were derived, both for the box in the upper and lower layers. Similarly, the incidence wave potentials were derived both for the surface and internal waves. These potentials were used to solve the diffraction problem for either the box is floating in the upper or lower layer of a two-layer fluid of finite depth. In calculating the wave exciting forces on the box, the internal wave influences were observed. This was done by varying the density ratio of the fluid. It was found that the density ratio greatly affects the wave exciting forces in a stratified fluid of constant depth. At large frequencies, the internal waves are of no importance in the predictions. However, there are influences of internal waves at relatively low frequencies. Conversely, when the layers have equal densities, then the two-layer fluid reduces to a single layer fluid, and the numerical results converge.

On the other hand, it was observed that the interface greatly affects the wave force. The height of the fluid was fixed and the depths of the layers were varied to demonstrate this phenomenon. When the interface changed, the numerical results were as expected for the shallow water effects on the wave force. However, the internal wave influences were still on course in the predictions.

Generally, internal waves and interfaces are of great influence to the wave forces and hydrodynamics of a body performing in stratified fluids. Therefore, there is need for them to be considered in the marine engineering designs and constructions.

ACKNOWLEDGEMENTS

The research done in the present work was supported by the National Natural Science Foundation of China (No. 11102049). It was also supported by The LRET through the joint center involving University College London, Shanghai Jiaotong University and Harbin Engineering University of which the authors are grateful.

REFERENCES

Endo H (1987). Shallow-water effect on the motions of three–dimensional bodies in waves. J. Ship Res. 31(1):34-40.

Grue J, Jensen A (2006). "Experimental velocities and accelerations in very steep wave events in deep water", Eur. J. Mech. B/Fluids 25(5):554-564.

Grue J, Jensen A, Rusas P, Sveen JK (1999). "Properties of large-amplitude internal waves", J. Fluid Mech. 380(1):257-278.

Hess JL, Smith AMO (1964). Calculation of nonlifting potential flow about arbitrary three-dimensional bodies. J. Ship Res. 8(2):22-44.

Kashiwagi M, Ten I, Makoto Y (**2006).** Hydrodynamics of a body floating in a two-layer fluid of finite depth, Part II. diffraction problem. J. Mar. Sci. Technol. 11(3):150-164.

Lu DQ, Chen TT (2009). Surface and interfacial gravity waves induced by an impulsive disturbance in a two-layer inviscid fluid. J. Hydrodynam. 21(1):26-33.

Manyanga DO, Duan WY (2011a). "Three Dimensional Internal Waves due to Pulsating Sources and Oscillation of Floating Bodies",

presented at the Proc. 6th Int. Conf. Fluid Mech. China 1376:265-267.
Manyanga DO, Duan WY (2011b). "Green functions with pulsating sources in a two-layer fluid of finite depth", China Ocean Eng. 25(4):609-624.
Manyanga DO, Duan WY (2012). Internal Wave Propagation from Pulsating Sources in a Two- layer Fluid of Finite Depth. J. Appl. Mech. Mater. 201-202:503-507. Trans Tech Publications, Switzerland.
Mohapatra S, Bora SN (2008). Water wave interaction with a sphere in a two-layer fluid flowing through a channel of finite depth. Arch. Appl. Mech. 79:725-740.
Nguyen TC Yeung RW (2010). Unsteady three-dimensional sources for a two-layer fluid of finite depth and their applications. J. Eng. Math. 70(1-3):67-91.
Ten I, Kashiwagi M (2004). Hydrodynamics of a body floating in a two-layer fluid of finite depth. Part I. Radiation problem $\left[J \right]$ J. Mar. Sci. Technol. 9(3):127-141.
Ying G, Xiu-jia C, Teng B (2012). A time-domain boundary element method for wave diffraction in a two-layer fluid. J. Appl. Math. 2012(2012):15.

APPENDIX

Integration scheme

The integration on a panel was carried out by the method of Hess and Smith (1964). In this case, the velocity potential is assumed to be constant over the panel. So, this method is used by applying a plane quadrilateral panel on a collocation point P. The coordinates of the corners of the quadrilateral ($(x_1, y_1, z_1), (x_2, y_2, z_2), (x_3, y_3, z3_3), (x_4, y_4, z_4)$) are transformed into a square standard region for easy calculation. On the other hand, the surface $P(x, y, z)$ can be expressed in the surface $Q(\xi, \eta, \zeta)$ by the transformation:

$$x = \sum_{i=1}^{4} N_i(\xi, \eta) x_i \; ; \qquad y = \sum_{i=1}^{4} N_i(\xi, \eta) y_i \; ; \qquad z = \sum_{i=1}^{4} N_i(\xi, \eta) z_i \qquad \text{(Ap.1)}$$

where

$$N_1(\xi, \eta) = 0.25 \times (1-\xi)(1-\eta)$$

$$N_2(\xi, \eta) = 0.25 \times (1-\xi)(1+\eta)$$

$$N_3(\xi, \eta) = 0.25 \times (1+\xi)(1+\eta)$$

$$N_4(\xi, \eta) = 0.25 \times (1+\xi)(1-\eta)$$

Therefore, integration on a quadrilateral can be performed by transforming a function $f(x, y, z)$ into the function $f(\xi, \eta, \zeta)$ in the following manner:

$$\iint_S f(x, y, z)\, ds = \iint_{S'} f(\xi, \eta, \zeta) \left| J \right| ds' \qquad \text{(Ap.2)}$$

where $\left| J \right|$ is the Jacobian of the transformation given by:

$$J = \begin{vmatrix} \hat{i} & \hat{j} & \hat{k} \\ \dfrac{\partial x}{\partial \xi} & \dfrac{\partial y}{\partial \xi} & \dfrac{\partial z}{\partial \xi} \\ \dfrac{\partial x}{\partial \eta} & \dfrac{\partial y}{\partial \eta} & \dfrac{\partial z}{\partial \eta} \end{vmatrix} \qquad \text{(Ap.3)}$$

Denoting the following components,

$$I_1 = \frac{\partial y \partial z}{\partial \xi \partial \eta} - \frac{\partial y \partial z}{\partial \eta \partial \xi} ; \; I_2 = \frac{\partial x \partial z}{\partial \xi \partial \eta} - \frac{\partial x \partial z}{\partial \eta \partial \xi} ; \; I_3 = \frac{\partial x \partial y}{\partial \xi \partial \eta} - \frac{\partial x \partial y}{\partial \eta \partial \xi} ,$$

Then

$$\left|J\right| = \sqrt{I_1 + I_2 + I_3} \qquad \text{(Ap.4)}$$

Thus we can now evaluate the integral (Ap.2) numerically by applying Gauss-Legendre quadrature:

$$\iint_{S'} f(\xi,\eta,\zeta)\left|J\right| ds' = \sum_{i}^{N_i}\sum_{j}^{N_j} w_{ij}\, f_{ij}(\xi,\eta,\zeta)\left|J\right| \qquad \text{(Ap.5)}$$

where w_{ij} are the weight functions of the N points. In the present work, a 4-point Gaussian rule has been employed. However, it has been found that using higher order Gaussian rule does not change much the predictions of the hydrodynamic coefficients. Hence, this low order rule is used and the advantage is that it drastically saves computation time.